Cell

Dissecting Spindle Architecture with a Laser

Pierre Recouvreux[1] and Marileen Dogterom[1,*]
[1]FOM Institute AMOLF, Science Park 104, 1098 XG Amsterdam, The Netherlands
*Correspondence: dogterom@amolf.nl
DOI 10.1016/j.cell.2012.04.006

Microtubules in spindles are too dense to resolve by light microscopy, even with super-resolution methods. Using a new method based on laser-ablation techniques, Brugués et al. present the first quantitative characterization of the vertebrate meiotic spindle and propose an assembly mechanism for building this architecture.

In eukaryotes, chromosome segregation is achieved by mitotic or meiotic spindles. These spindles are complex dynamic structures composed of microtubules and associated proteins. Although the mechanisms by which spindles are assembled have received considerable interest, a detailed description of the microtubule organization within the spindle is lacking, hampering a detailed understanding of how spindle assembly is controlled. The problem is that the high density of microtubules, in general, does not allow for a quantitative analysis by fluorescence microscopy, and electron microscopy cannot easily cope with the high number of microtubules. In this issue of *Cell*, Brugués et al. (2012) present a clever, innovative method to derive structural information from laser-cutting experiments on meiotic spindles in *Xenopus laevis* egg extracts. The result is a quantitative description of microtubule architecture within a large, metazoan spindle, including the polarity and length distributions of the microtubules within the spindle. By combining the experimental results with a model of spindle dynamics, the authors propose an assembly mechanism that involves inhomogeneous nucleation of microtubules and transport of the microtubules toward the spindle's poles.

Laser ablation or laser cutting is a technique that has been used to obtain information about force generation or contractility in living cells. For example, Grill and coworkers used a UV laser to create breaks in microtubules in dividing *Caenorhabditis elegans* zygotes, which uncovered cortical pulling forces on the spindle (Grill et al., 2001). More recently, this laboratory cut the actomyosin cortex in order to probe the distribution of cortical tension (Mayer et al., 2010). In another study, Khodjakov and coworkers used a green laser to cut the mitotic spindles of fission yeast cells (Khodjakov et al., 2004), thereby revealing information about the mechanisms underlying spindle elongation. These studies focused on morphological changes of cytoskeleton networks upon laser ablation but did not provide any structural information.

In their new article, Brugués et al. take advantage of a high-intensity pulsed laser to perform laser cutting on microtubules in dense meiotic spindles. They obtain detailed information on the organization of microtubules based on a simple observation: the cut made in a single microtubule creates two new ends of opposite polarity, which subsequently exhibit different behavior (Figure 1A). Whereas the newly formed minus end remains stable, the new plus end quickly depolymerizes, which leads to the eventual disappearance of this fragment. This shrinkage event is directed toward the old minus end of the microtubule, indicating its orientation. Performing a laser cut on a complete spindle induces two depolymerization waves as a result of the two possible orientations of microtubules along the spindle axis.

A detailed analysis of the loss in fluorescence associated with the depolymerization fronts (Figures 1B and 1C) allows Brugués et al. to determine the organization of microtubules in the spindle. By comparing the intensity of the two waves immediately after the cut, the local polarization of the microtubule network can be estimated. The authors then show that the middle of the spindle contains an equal number of microtubules pointing in both directions, but near the poles, most of the microtubules have their plus ends pointing away from the pole. Furthermore, the progressive decay in the depolymerization front reveals the locations of the minus ends; this gives a quantitative measure of the density of minus ends that belong to microtubules that have been cut at a certain position in the spindle.

Although these measurements offer important information, they alone cannot provide quantitative data on microtubule length distributions within the spindle. To accomplish this, Brugués and colleagues use a clever trick: they perform two laser cuts at nearby locations in the spindle. The comparison between the subsequent depolymerization waves allows a quantitative measure of the density of plus ends between the two cuts. Together with information on the locations of minus ends, these data reveal the length distribution of microtubules: microtubules with their plus ends pointing away from the pole are, on average, short near the poles and long when farther away from the poles.

The authors then turn to theoretical modeling to help explain the observed spindle architecture. They discuss two simplified mechanisms, which both involve a collection of microtubules that can be nucleated throughout the spindle and then transported at a constant rate in the direction of their minus ends. Newly nucleated microtubules grow until they

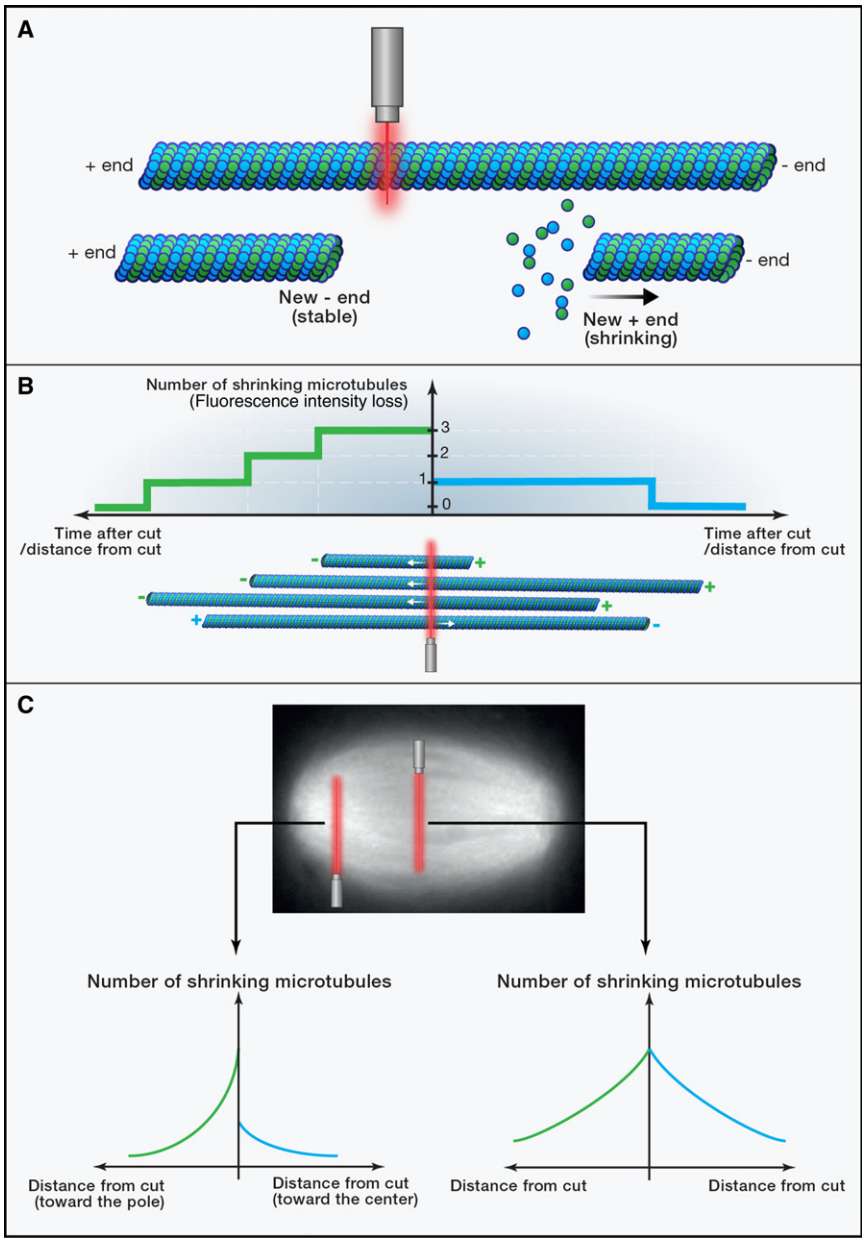

Figure 1. Laser Cuts Create Depolymerization Fronts that Reveal Spindle Architecture

(A) When a single microtubule is cut by a high-intensity laser pulse, two new ends with opposite polarities are created. The new minus end is stable, whereas the new plus end quickly depolymerizes until the microtubule fragment completely disappears. Laser cutting, thus, produces a depolymerization front propagating toward the original minus end; this is detected by a loss of fluorescence.

(B) In a collection of parallel microtubules, laser cutting creates two depolymerization fronts. The subsequent loss of fluorescence on the left and right sides of the cut gives a measure for the local number of shrinking microtubules that have their minus ends located at the left and right sides of the cut, respectively. In this example, there are three minus ends located on the left side and one minus end located on the right side. The ratio of the fluorescence intensity loss around the cut reveals the polarity of the network. As the depolymerization fronts move away from the cut, the total number of microtubules contributing to the intensity loss decreases each time a shrinking microtubule reaches its minus end. This decay, therefore, directly reveals where minus ends are located. By comparing the results of two nearby cuts, it is also possible to "count" the number of plus ends located between these cuts (not shown).

(C) Brugués et al. (2012) find that the shapes of the depolymerization fronts depend on the position of the cut within the spindle. In the center of the spindle, the depolymerization fronts are symmetrical: the numbers of microtubules pointing in each direction are the same. Close to the pole, the asymmetry in the two fronts indicates that most microtubules point with their minus ends toward the pole (green curve).

experience a random catastrophe event (with a probability determined by the local catastrophe rate), after which they shrink and disappear. In the first scenario, called the "stability model," short microtubules at the poles are assumed to be the result of a high local catastrophe rate. In this model, unstable microtubules near the poles do not become as long as microtubules near the center of the spindle, which have a low catastrophe rate. In the second scenario, called the "nucleation model," the catastrophe rate is assumed constant, but the nucleation rate is allowed to vary over the length of the spindle. In this model, a peak in the nucleation rate close to the center of the spindle, combined with transport of the microtubules toward to the poles, leads to an excess of short, shrinking microtubules near the spindle poles. Although this last scenario is not as intuitive as the first, both scenarios are numerically shown to be consistent with the observed profile of average microtubule lengths. However, each has clearly different predictions about where in the spindle growing ends are preferentially found and where most tubulin incorporation is therefore taking place. A separate measurement of these parameters clearly reveals an excess of growing plus ends in the center of the spindle, favoring the "nucleation model."

Of course, it is possible, maybe even likely, that the situation in the spindle is not as black and white as concluded from comparing these two scenarios. Dynamic parameters that vary spatially (or molecules that cut microtubules, such as katanin; Loughlin et al., 2011) may also contribute to the eventual architecture of the spindle. Nevertheless, these combined modeling and experimental results convincingly show that, to explain the spatially varying distribution of microtubule lengths, it is sufficient to consider a spatially varying nucleation rate, but it is not sufficient to consider a spatially varying stability of the microtubules. The remaining issue then becomes to understand the mechanism by which

The fast decay toward the pole further shows that there is a local high density of minus ends near the poles. Together with information on the location of plus ends (not shown), the data indicate that microtubules are shorter close to the poles and longer in the middle of the spindle.

microtubule nucleators are distributed inhomogeneously. Two mechanisms, which are not mutually exclusive, have been proposed to date: a gradient of nucleators around chromatin (Caudron et al., 2005) and a microtubule-mediated nucleation process (Clausen and Ribbeck, 2007). In the future, the approach presented in this study—that is, combining innovative experimental techniques with mathematical modeling and simulations (Loughlin et al., 2010)—may prove to be helpful to investigate this question.

ACKNOWLEDGMENTS

M.D. is supported by a NWO-ALW VICI grant and by the Stichting voor Fundamenteel Onderzoek der Materie (FOM), which is financially supported by the Nederlandse organisatie voor Wetenschappelijk Onderzoek (NWO).

REFERENCES

Brugués, J., Nuzzo, V., Mazur, E., and Needleman, D.J. (2012). Cell *149*, this issue, 554–564.

Caudron, M., Bunt, G., Bastiaens, P., and Karsenti, E. (2005). Science *309*, 1373–1376.

Clausen, T., and Ribbeck, K. (2007). PLoS ONE *2*, e244.

Grill, S.W., Gönczy, P., Stelzer, E.H.K., and Hyman, A.A. (2001). Nature *409*, 630–633.

Khodjakov, A., La Terra, S., and Chang, F. (2004). Curr. Biol. *14*, 1330–1340.

Loughlin, R., Heald, R., and Nédélec, F. (2010). J. Cell Biol. *191*, 1239–1249.

Loughlin, R., Wilbur, J.D., McNally, F.J., Nédélec, F.J., and Heald, R. (2011). Cell *147*, 1397–1407.

Mayer, M., Depken, M., Bois, J.S., Jülicher, F., and Grill, S.W. (2010). Nature *467*, 617–621.

Dialing Down SUN1 for Laminopathies

Yousin Suh[1,2,*] and Brian K. Kennedy[2,3,*]
[1]Departments of Genetics and Medicine, Albert Einstein College of Medicine, Bronx, NY 10461, USA
[2]Aging Research Institute, Guangdong Medical College, Dongguan 523808, Guangdong, China
[3]Buck Institute for Research on Aging, Novato, CA 94945, USA
*Correspondence: yousin.suh@einstein.yu.edu (Y.S.), bkennedy@buckinstitute.org (B.K.K.)
DOI 10.1016/j.cell.2012.04.003

Laminopathies, caused by mutations in A-type nuclear lamins, encompass a range of diseases, including forms of progeria and muscular dystrophy. In this issue, Chen et al. provide evidence that elevated expression of the nuclear inner membrane protein SUN1 drives pathology in multiple laminopathies.

Since their initial link to human disease, A-type nuclear lamins have been the subject of intense scrutiny. Mutations, mostly missense ones, in *LMNA*, the gene that encodes all A-type lamins by alternative splicing (lamins A and C are the most prominent), cause diseases ranging from dystrophic syndromes (including forms of muscular dystrophy, lipodystrophy, and dilated cardiomyopathy) to progeroid disorders such as Hutchinson-Gilford progeria syndrome (HGPS), which present with a rapid onset of a subset of pathologies that are associated with normal aging (Burtner and Kennedy, 2010). Why do different mutations in a structural component of the nucleus cause such an array of debilitating disorders?

Mouse models of a wide spectrum of laminopathies have been developed, ranging from a knockout of the *LMNA* gene, which dies at 6–8 weeks of age with dilated cardiomyopathy and skeletal muscle dystrophy (Sullivan et al., 1999), to mice engineered to express human disease mutations (Cohen and Stewart, 2008). The models generally recapitulate their respective human disease phenotypes and serve to uncover mechanisms underlying pathophysiology and disease progression. As a starting point for the study by Chen et al. (2012), a double-knockout mouse was created lacking both A-type lamins and SUN1. SUN1 interacts with lamin A/C as components of the linker of nucleoskeleton and cytoskeleton (LINC) complex, which mediates crosstalk between the actin cytoskeleton and the nucleus, leading to large-scale nuclear movements within the cell (Meinke et al., 2011). The expectation was that loss of SUN1 would exacerbate the already severe skeletal muscle and cardiac phenotypes in the *Lmna* knockout, but to the authors' surprise, the reverse was true. The $Lmna^{-/-}$ $Sun1^{-/-}$ mice survive significantly longer than $Lmna^{-/-}$ single knockouts, resisting a range of $Lmna^{-/-}$ pathologies, including lordokyphosis, growth defects, reduced bone density, and cardiac/skeletal muscle defects (Figure 1; Chen et al., 2012).

There was already reason to believe that the LINC complex might be linked to laminopathies, as mutations in another LINC component, Emerin, cause Emery-Dreifuss muscular dystrophy. Loss of A-type lamins leads to mislocalization of other LINC components (Vaughan et al., 2001, Muchir et al., 2003), but prior to this study, it was not known how SUN1 would be affected. In embryonic fibroblasts from $Lmna^{-/-}$ mice, Chen et al. make two important observations—first that SUN1 is highly overexpressed and second that a substantial portion of the